iScience

CellPress
OPEN ACCESS

Article

Efficient and durable uranium extraction from uranium mine tailings seepage water via a photoelectrochemical method

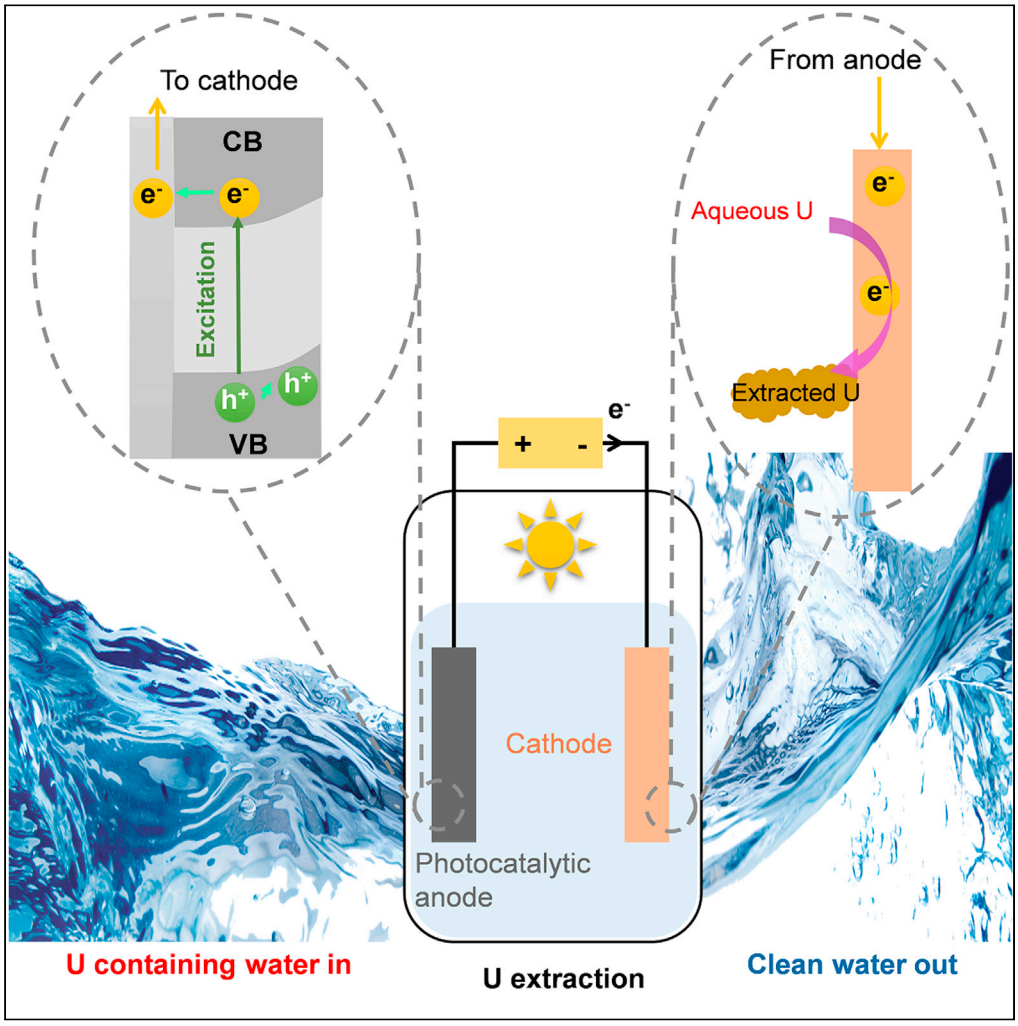

Yin Ye, Jian Jin, Yanru Liang, ..., Yanlong Chen, Fan Chen, Yuheng Wang

yeyin01@hotmail.com, yin.ye@nwpu.edu.cn (Y.Y.)
chenfanhit@163.com (F.C.)
yuheng.wang@nwpu.edu.cn (Y.W.)

Highlights

Efficient and durable U extraction by a photoelectrochemical method

Spatial separation of charge carriers is achieved by the applied bias potential

Stable pentavalent U is produced under ambient conditions

The proposed photoelectrochemical method is economically feasible

Ye et al., iScience 24, 103230
November 19, 2021
https://doi.org/10.1016/j.isci.2021.103230

iScience

CellPress
OPEN ACCESS

Article

Efficient and durable uranium extraction from uranium mine tailings seepage water via a photoelectrochemical method

Yin Ye,[1,5,*] Jian Jin,[1] Yanru Liang,[1] Zemin Qin,[1] Xin Tang,[1] Yanyue Feng,[2] Miao Lv,[3] Shiyu Miao,[4] Cui Li,[1] Yanlong Chen,[1] Fan Chen,[1,*] and Yuheng Wang[1,*]

SUMMARY

Current photocatalytic uranium (U) extraction methods have intrinsic obstacles, such as the recombination of charge carriers, and the deactivation of catalysts by extracted U. Here we show that, by applying a bias potential on the photocatalyst, the photoelectrochemical (PEC) method can address these limitations. We demonstrate that, owing to efficient spatial charge-carriers separation driven by the applied bias, the PEC method enables efficient and durable U extraction. The effects of multiple operation conditions are investigated. The U extraction proceeds via single-step one-electron reduction, resulting in the formation of pentavalent U, which can facilitate future studies on this often-overlooked U species. In real seepage water the PEC method achieves an extraction capacity of 0.67 gU $m^{-3} \cdot h^{-1}$ without deactivation for 156 h continuous operation, which is 17 times faster than the photocatalytic method. This work provides an alternative tool for U resource recovery and facilitates future studies on U(V) chemistry.

INTRODUCTION

Nuclear power, fueled by uranium (U), is a mature low-carbon energy technology that plays a crucial role in the transition to a sustainable future (Rhodes, 2017; Cui et al., 2020b; Wang et al., 2020). Along with its rapid expansion, public concerns regarding its sustainability have arisen. One is the environmental impact, as billions of tons of U mine tailings have been disposed worldwide owing to mining and processing of U ores (Dang et al., 2018). Untreated, these tailings derive large quantities of U-containing (mg/L level) seepage waters (Dang et al., 2018). As U is highly hazardous to the biosphere, the seepage water would threaten the ecosystem if not properly treated (Bourrachot et al., 2014; Zheng et al., 2020; Zhang et al., 2019). Another concern is the vulnerability of the global U supply. Current U supply relies on terrestrial ores, which have limited availabilities and could hardly meet the future demand (Yuan et al., 2021; Liu et al., 2017; Tsouris, 2017; Lively, 2016; Cui et al., 2021b). Hence, recovering U from the seepage water is highly appealing because it simultaneously addresses the depletion of conventional uranium resources and the negative environmental impact of U mining.

Photocatalysis (PC) is a plausible approach for U extraction from aqueous media (Li et al., 2019c). The core processes of the PC U extraction method are the adsorption and reduction of soluble hexavalent U (U(VI)), which is the dominant U species in aquatic environment, into insoluble lower-valent U by conduction band electrons generated within the photocatalyst upon illumination. Currently, most research efforts have focused on developing novel photocatalysts (Liang et al., 2020; Deng et al., 2019), but two intrinsic obstacles persist (Figure 1A): the fast recombination of charge carriers upon their formation(Lianos, 2017),and the blockage of catalyst active sites by precipitated U (Li et al., 2017; Deng et al., 2019). Consequently, the efficiency of the PC method is limited, and catalyst regeneration is required, which hinders the long-term continuous operation. Suppressing the recombination of charge carriers and spatially separating the uranium deposition sites from photocatalyst active sites are the keys to tackle these challenges.

Here we show that the photoelectrochemical (PEC) method could effectively resolve the aforementioned drawbacks of PC methods. By applying a bias potential on the photocatalyst (Figure 1B), the PEC method enables much faster U extraction with exceptional stability, compared with the PC method operating under identical conditions. In real seepage water, the PEC method achieved a capacity of 0.67 gU $m^{-3} \cdot h^{-1}$

[1]School of Ecology and Environment, Northwestern Polytechnical University, 710129 Xi'an, P. R. China

[2]Department of Chemistry and Chemical Engineering, Chalmers University of Technology, 41296 Gothenburg, Sweden

[3]State Key Laboratory of Urban Water Resource and Environment, School of Environment, Harbin Institute of Technology, Harbin 150090, China

[4]College of Eco-Environmental Engineering, Qinghai University, Xining 810016, P. R. China

[5]Lead contact

*Correspondence: yeyin01@hotmail.com, yin.ye@nwpu.edu.cn (Y.Y.), chenfanhit@163.com (F.C.), yuheng.wang@nwpu.edu.cn (Y.W.)

https://doi.org/10.1016/j.isci.2021.103230

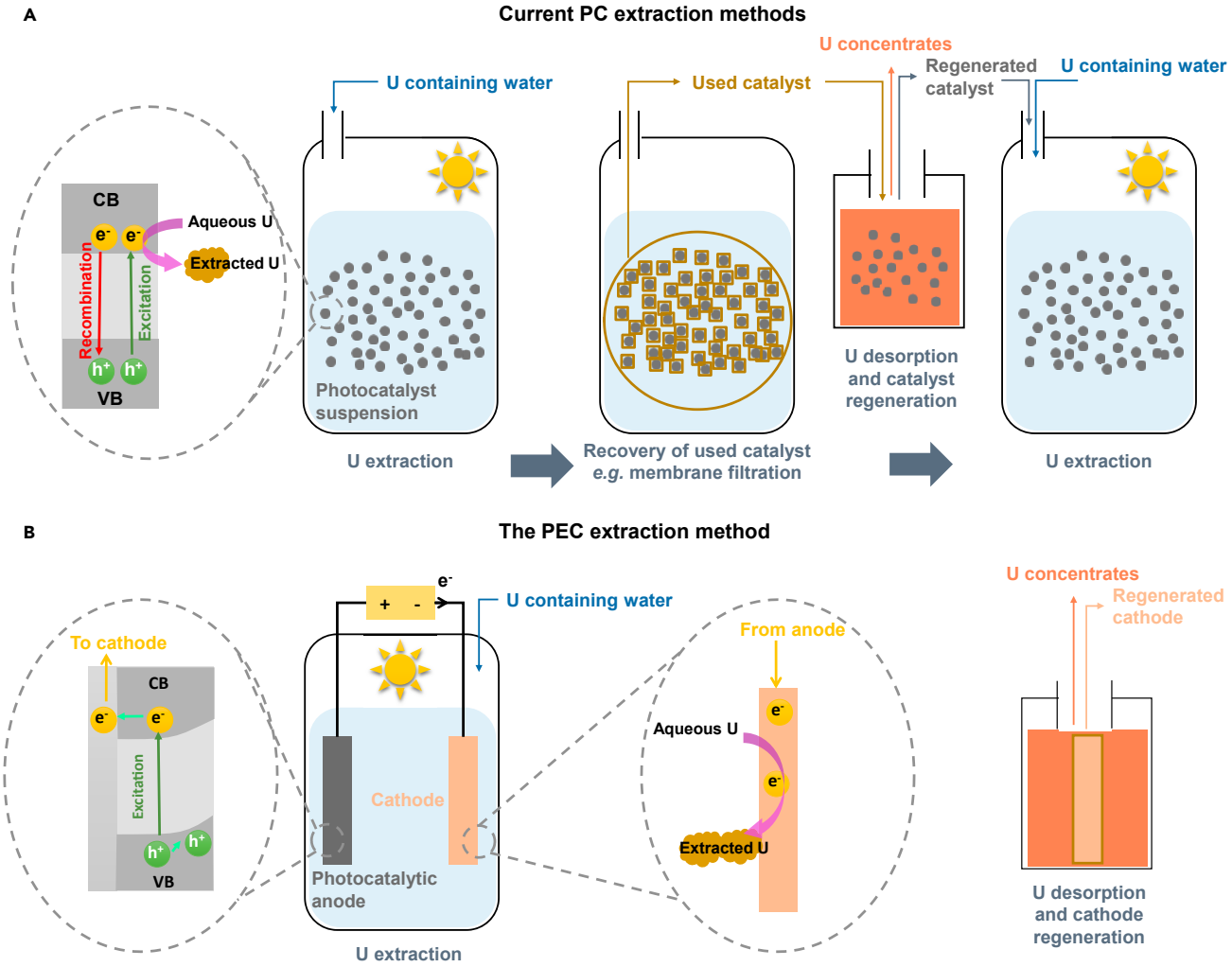

Figure 1. Schematic representations of different uranium extraction methods

(A) The PC uranium extraction method.

(B) The PEC uranium extraction method.

without further optimization, which is 17 times faster than the photocatalytic method using identical photocatalyst, at a compulsory energy cost of 125 kWh/kgU ($15.63/kgU). We further show that the bias-driven spatial charge-carriers separation is the key to obtain fast U extraction and high stability. The PEC U extraction proceeds via single-step one-electron reduction. For the first time we produced stable U(V) from aqueous media under ambient conditions without using organic ligands, implying the potential of the PEC method for facile U(V) synthesis, which would significantly facilitate future studies on U(V) chemistry. In summary, our work opens an appealing avenue for obtaining nuclear fuel and reducing the environmental footprint of U mines, contributing to the sustainability of the nuclear power industry.

RESULTS

The PEC U extraction method

We hypothesize that the key to obtaining higher efficiency and stability in PEC uranium extraction is the application of a proper external bias potential on the photocatalyst that can suppress the recombination of charge carriers and spatially separate the U deposition sites from the photocatalyst active sites. To examine this hypothesis, PEC experiments were conducted at varied bias potentials with synthetic U-containing water. Control experiments were also performed with illumination at open-circuit condition (i.e., PC U extraction) and in the dark with external bias (i.e., EC U extraction). The experimental setup

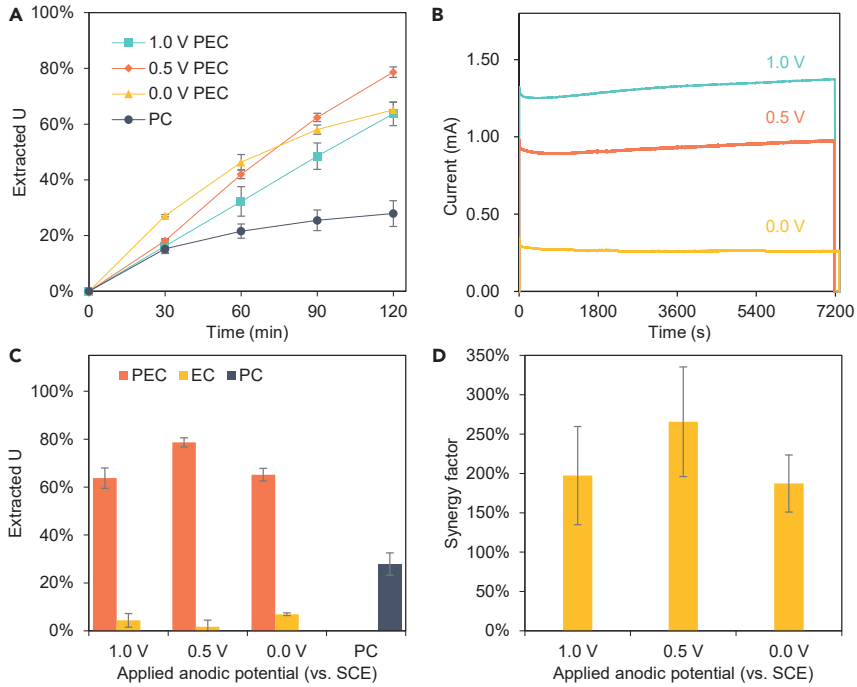

Figure 2. Performance of the PEC uranium extraction method

(A) Time-resolved uranium extraction performance by the PEC method and the PC method.

(B) The current-time plots during PEC U extraction experiments.

(C) Total U extraction efficiencies of different methods after 120 min operation.

(D) The synergy factors of the PEC method at varied bias potentials. Conditions: $[U(VI)]_0$ = 0.05 mM, [NaCl] = 20 mM, natural pH (~4.2). The error bars represent the standard deviation between replicates.

consisted of a TiO_2 nanotube array (TNA) photoanode and a Ti foil cathode. TiO_2 is the most developed and most commonly used photocatalyst (Yang et al., 2008), and its conduction band edge potential is suitable for U(VI) reduction (Li et al., 2017). Moreover, among various immobilized TiO_2 for photoelectrocatalysis purposes, TNA is considered to be a viable catalyst because of its large specific surface area, high stability, and unique charge carriers transport properties (Wang et al., 2014). The Ti foil was used as the cathode, because its capability of serving as the U deposition site has been demonstrated in previous electrochemical uranium extraction studies (Liu et al., 2019).

Fast PEC U extraction kinetics were obtained at all tested bias potentials, and the total extraction efficiencies after 120 min operation reached 65.2%, 78.7%, and 63.8%, at applied bias potential of 0.0 (all potentials reported in this work are relative to the standard calomel electrode [SCE] unless otherwise stated), 0.5, and 1.0 V, respectively (Figures 2A and 2C). In the case of PC method, U extraction was much slower, where a total efficiency of 28.9% was achieved after 120 min operation. The results implied a significant role of the applied bias in promoting the U extraction efficiency of the PEC method.

By comparing the U extraction efficiencies of the EC, PC, and PEC methods, obvious synergistic effects were observed in the PEC method: the synergy factor at 0.0, 0.5, and 1.0 V were 187%, 266%, and 197%, respectively, calculated according to previous studies (Kim et al., 2015) (Figure 2D). The bias potential might play two roles in PEC U extraction. One is driving direct EC U extraction on electrode surfaces (Liu et al., 2019; Kim et al., 2015). However, the dark control experiments showed insignificant U extraction ($\lesssim$7%) at all tested bias potentials (Figures 2C and S2), indicating a minor contribution of the direct EC U extraction. The other role of the bias potential is promoting the separation of charge carriers by triggering band bending within the photocatalyst (Mazierski et al., 2019). In TiO_2-based photoelectrochemical processes, when the applied bias potential is greater than the flat-band potential of TiO_2, band bending to the positive direction within TiO_2 will be generated (Radecka, 2004; Zhang and Yates, 2012; Feng et al., 2020). Consequently, upon illumination and excitation, conduction band electrons would migrate to the

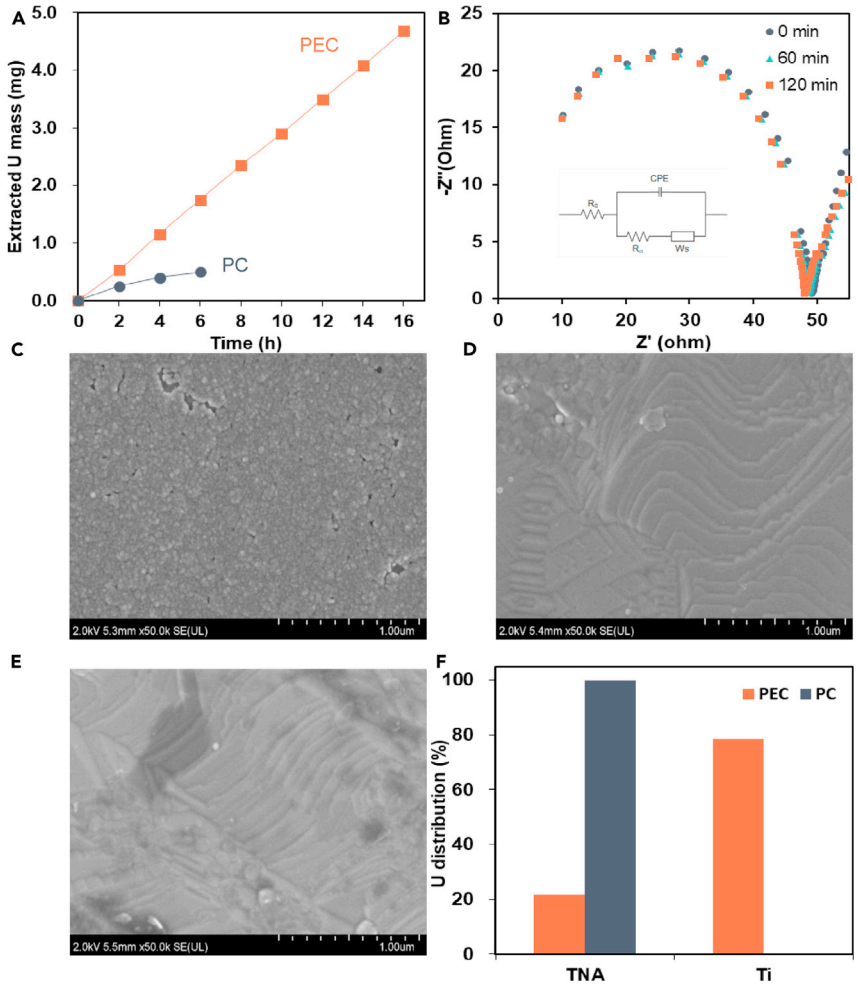

Figure 3. Durability of the PEC system

(A) The performances of the PEC method and the PC method during continuous cyclic runs.

(B) *In situ* EIS plots of the Ti electrode during the PEC uranium extraction experiment.

(C) SEM image of the Ti electrode after PEC uranium extraction.

(D) SEM image of the Ti electrode after PC uranium extraction.

(E) SEM image of the fresh Ti electrode.

(F) Comparison of the uranium content on different electrodes after PEC and PC uranium extraction operation.

Conditions: $[U(VI)]_0$ = 0.05 mM, unadjusted pH (~4.2), [NaCl] = 20 mM, E_{bias} = 0.50 V versus SCE.

counter electrode (Ti electrode in this case) through the external circuit driven by the potential difference between the photoanode and the counter electrode. In this way, the spatial separation of the charge carriers is achieved and the recombination of charge carriers is reduced, resulting in promoted efficiencies (Mazierski et al., 2019). In the PEC U extraction experiments, the applied bias potentials were greater than the flat-band potential of TiO_2 (−0.2 to −0.4 V) (Radecka, 2004), so it is reasonable to expect the effective separation of charge carriers. This was evidenced by the increased photocurrent with the increasing bias potential during PEC U extraction (Figure 2B). Furthermore, although the photocurrent increased with higher bias potential, an optimal value exists. This might be attributed to the production of oxidative species at a higher potential that can re-oxidize the precipitated U.

During the PEC U extraction, as the photocurrent (Figure 2B) indicates constant extraction of conduction band electrons from the photocatalyst to the cathode, the U deposition sites and the photocatalyst should be spatially separated; therefore, higher stability and durability of the photocatalyst are expected. To test this expectation, we performed a reusability assay (Figure 3A). After each cycle, defined reaction solutions were directly refilled into the PEC reactor and the PC reactor without regeneration treatment of the TiO_2

nanotube array (TNA) and the Ti electrode. The PEC method indeed showed high durability, as ~0.58 mg U could be extracted from 0.06 L synthetic U-containing water for each of the eight tested 120-min operation cycles. On the contrary, in the first cycle of the PC method, only 0.28 mg U was extracted, and the extracted U decreased to 0.15 and 0.10 mg during the second and the third cycles, respectively. Hence, the PEC method had exceptional stability compared with the PC method. For the spatial separation of the U deposition sites and photocatalyst, the role of the applied bias potential on the photocatalyst is crucial, because it determines the direction of the electron flow. The effective spatial separation of the U deposition sites and photocatalyst observed in the present study can be ascribed to the positive band bending (resulting in extraction of electrons out of the photocatalyst) induced by the applied bias potential that was more positive than the flat-band potential of TiO_2 (Radecka, 2004; Zhang and Yates, 2012; Feng et al., 2020). On the contrary, spatial separation of U deposition sites and the photocatalyst cannot be achieved by the application of a bias potential that is more negative than the flat-band potential of the photocatalyst, because the positive band bending cannot be established at such a potential (Kim et al., 2015).

The morphologies of the Ti electrodes upon 120-min PEC and PC U extraction experiments were characterized by scanning electron microscopy (SEM) and compared with that of the fresh Ti electrode. The results show that, upon PEC treatment, the electrode was covered by a nanoparticles layer (Figures 3C and 3E), which contains U according to energy dispersive spectroscopy (EDS) analysis (Figure S4). However, in the case of PC U extraction, no noticeable changes in the electrode morphology (Figures 3D and 3E) or U deposition (Figure S5) was observed. We further analyzed the distribution of extracted U on both the TNAs and the Ti electrodes upon PC and PEC experiments. The results revealed that, in the case of PC, U extraction products were precipitated exclusively on the TNA photocatalyst (Figures 3F and S6), which confirmed that the blockage of the photocatalyst active sites by extracted U was responsible for the poor stability of the PC U extraction technology (Li et al., 2017, 2019a; Deng et al., 2019). On the contrary, extracted U was predominantly (78.4%) precipitated on the Ti cathode in the case of PEC (Figure 3F), even though a small fraction was found on the TNA photocatalyst, most probably as adsorbed species (Bonato et al., 2012). Therefore, the spatial separation of the U precipitation sites and the photocatalyst could explain the stable photoactivity of the TNA photoanode and therefore the stable photoelectrons output in PEC method. More interestingly, the continuous U precipitation onto the Ti cathode in the PEC method did not decrease its U reduction capacity (Figure 3A). To clarify this aspect, *in situ* electrochemical impedance spectroscopy (EIS) analysis (Li et al., 2020) was carried out to monitor the interfacial charge transfer resistance changes in real time during the PEC U extraction. The curves shrank slightly during the experiment (Figure 3B), and the fit results revealed gradual decrease in interfacial charge transfer resistance of the Ti cathode (Table S1; Scheme S1), which could facilitate the U reduction. This finding was consistent with the slightly increasing pattern of the current during one cycle (Figures 2B and S3) and the similar currents among different continuous cycles (Figure S3). The results here suggested that the U precipitates on the Ti cathode could facilitate further U deposition, instead of blocking the active sites.

As the operation conditions may vary greatly among seepage waters from different U mines, the effects of different operation conditions on the performance of the PEC method were examined. We first evaluated the PEC uranium extraction performance at pH from 4.2 to 9.0. The results show that a similar U extraction rate in the first 60 min was achieved for all the tested pH values, whereas a lower rate was observed for higher pH at 60–120 min (Figure 4A). One plausible explanation would be the changes in the speciation of aqueous U(VI) with the increasing pH (Figure S7). At acidic pH (4.2), U(VI) was predominantly present as uranyl (UO_2^{2+}) ions, and the complexation of UO_2^{2+} with OH^- or CO_3^{2-} ions increased with the increasing pH (Kim et al., 2015). In the case of higher pH, as the U extraction proceeded, the residual aqueous U concentration decreased, so the proportion of UO_2^{2+}–OH^- and UO_2^{2+}–CO_3^{2-} complexes increased with the extraction time. Cyclic voltammetry (CV) curves of the Ti cathode in the synthetic U-containing water at various pH show that these UO_2^{2+}–OH^- and UO_2^{2+}–CO_3^{2-} complexes had more negative reduction potentials than UO_2^{2+} ions (Figure S8), implying that the reduction of these hydroxyl and carbonate complexes predominant at higher pH was less thermodynamically favorable. Moreover, as U reductive precipitation mostly took place on the Ti cathode, the adsorption of U(VI) to the Ti electrode surface should be a prerequisite for its reduction. In the case of higher pH, the electric repulse between the negatively charged UO_2^{2+}–OH^- and UO_2^{2+}–CO_3^{2-} species and the Ti cathode surface might also obstruct the U reduction.

Thereafter, we evaluated the PEC U extraction performance at different initial U concentrations ranging from 0.025 to 0.20 mM (Figures 4B and S9). The high initial U concentrations, i.e., 0.10 and 0.20 mM, enabled faster kinetics in the first 30 min. As for the low initial U concentrations, i.e., 0.025 and 0.05 mM, the

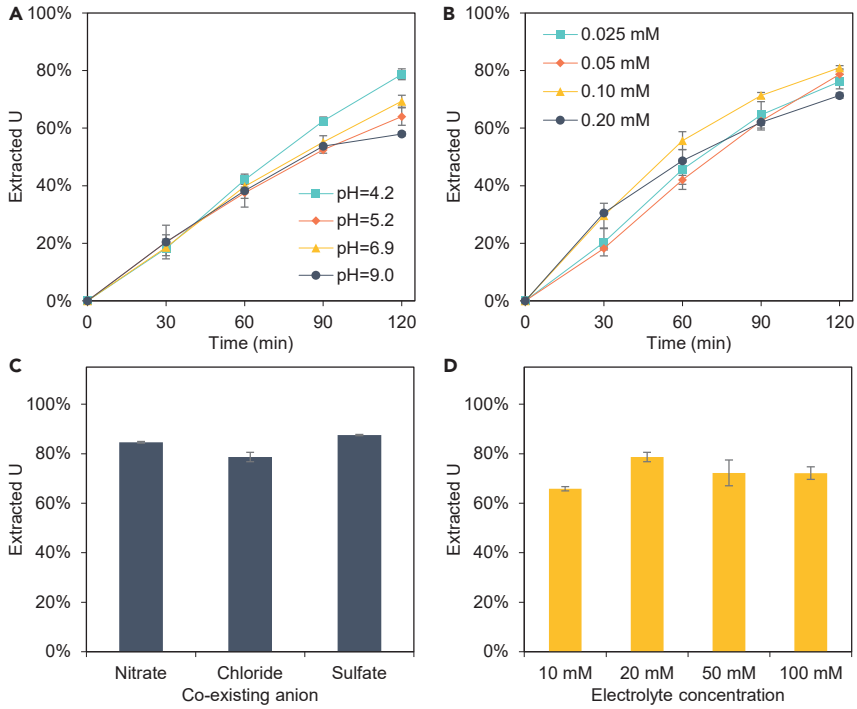

Figure 4. Effects of operation conditions on PEC uranium extraction

(A) PEC uranium extraction performance at varied pH.

(B) PEC uranium extraction performance at varied initial uranium concentration.

(C) PEC uranium extraction performance with the presence of different anions.

(D) PEC uranium extraction performance with different electrolyte concentrations. The error bars represent the standard deviation between replicates.

accumulation of U precipitates on the Ti cathode, which was beneficial for the extraction of aqueous U, was more difficult (Liu et al., 2019), so slower initial rates were obtained. But once some U precipitates were deposited, the extraction was accelerated and resulted in similar kinetics with high initial U concentrations in the later phase. In the case of the 0.20 mM U experiment, the extraction rate in the later phase declined and became the slowest, which might be due to the saturation of the active sites (Li et al., 2019b).

NO_3^- and SO_4^{2-} are abundant in many U mining effluents (Dlamini et al., 2019), so their effects on PEC methods were examined. The results show that slightly higher U extraction rates were obtained by replacing the 20 mM NaCl with 20 mM $NaNO_3$ or Na_2SO_4 in the synthetic U-containing water (Figure 4C). The speciation of aqueous U(VI) could be different in the presence of different anions, because of the different complexation abilities of different anions with U(VI). The electrochemical interactions of these different U(VI) complexes could vary greatly, which was evidenced by CV scans (Figure S10).

The conductivity of the aqueous media, which is correlated to the electrolyte concentration, may affect photoelectrochemical water treatment processes (Garcia-Segura and Brillas, 2017). To examine this aspect, PEC U extraction experiments were conducted at different electrolyte concentrations. The conductivity of the reaction solution was measured to be 1.27, 2.37, 5.55, and 10.76 mS/cm, when the concentration of NaCl was 10, 20, 50, and 100 mM, respectively. The results show that the extraction rate did not vary significantly while the electrolyte (NaCl) concentration increased dramatically from 10 to 100 mM (the conductivity of the reaction solution increased from 1.27 to 10.76 mS/cm) (Figure 4D). In typical (photo)electrochemical water treatment systems, the overall charge-carriers transfer resistance mainly consists of two components, i.e., the solution/ohmic resistance due to the resistance of the ions transfer in the reaction solution and the charge transfer barriers at the solution/electrode interfaces (Chen et al., 2016). The currents at varied NaCl concentrations (corresponding to varied conductivity and therefore varied solution/ohmic resistance) were similar (Figure S11), implying that charge transfer barriers at the electrode/solution interfaces dominated the charge transfer resistance in the tested NaCl concentration range.

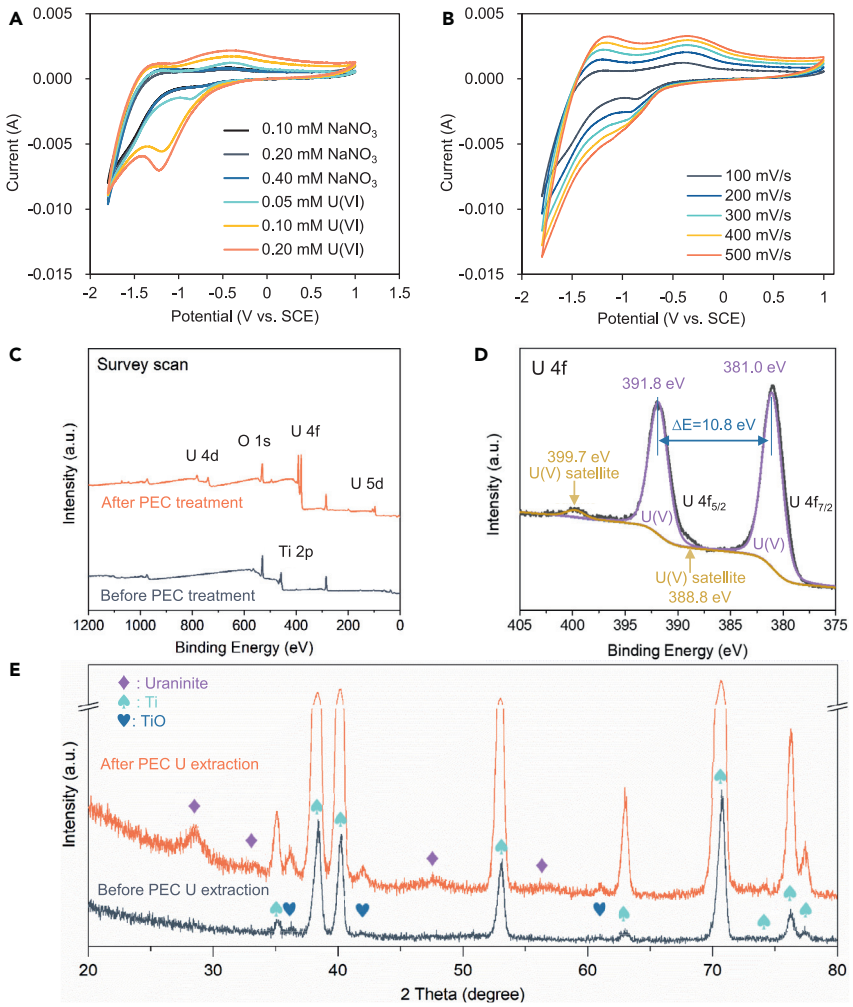

Figure 5. Mechanistic investigations

(A) Cyclic voltammograms of the Ti electrode in synthetic water with/without uranium, at a scan rate of 100 mV/s.

(B) Cyclic voltammograms of the Ti electrode in synthetic water with 0.05 mM uranium at varied scanning rate.

(C) XPS survey scan spectra of the Ti electrode before and after PEC uranium extraction.

(D) XPS U4f scan of the Ti electrode after PEC uranium extraction.

(E) XRD spectrum of the Ti electrode after PEC uranium extraction.

The geological conditions, climate conditions, and applied mining techniques differ significantly among U mines. Consequently, the pH, the concentration of U, the type of co-existing anions, as well as the conductivity in different mine tailings seepage waters can vary significantly (Dang et al., 2018). The results present herein imply that the PEC method has good compatibility with different water matrices and resilience to the variation of pH, U concentration, and co-existing anions in a broad range.

Mechanisms: formation of stable pentavalent U

To decipher the mechanisms governing the PEC U extraction processes, the electrochemical interactions of aqueous U and the Ti electrode were studied using CV, and the results are shown in Figures 5A and 5B. In the presence of U(VI), a reduction peak at around −0.85 V emerged. Meanwhile, an oxidation peak emerged at −0.36 V, in the presence of U(VI). Considering that no redox peaks were detected in the absence of U(VI), all these observed redox peaks can be assigned to the redox changes of U species on the Ti electrode. Furthermore, on increasing the scanning rate, the reduction peaks shifted to lower potentials, whereas the oxidation peaks moved to higher potentials (Figure 5B). These reflected the kinetics of the redox reactions (Yuan et al., 2015a). Linear relations between the reduction/oxidation peak current

values and the square root of scanning rates were identified (Figure S12), suggesting that both the reductive conversion and the oxidative conversion were diffusion-controlled reactions that could be described by the Randles-Sevcik model (Yuan et al., 2015a; Gao et al., 2017; Li et al., 2021). Fit with the Randles-Sevcik model, the CV data revealed a one-electron U(VI) reduction process on the Ti electrode (see Figure S14). Therefore, the reduction peaks at around −0.85 V versus SCE can be assigned to the one-electron reduction of U(VI) to pentavalent U (U(V)) (Liu et al., 2017; Kim et al., 2015; Hennig et al., 2010; Morris, 2002), and the oxidation peaks at −0.36 V versus SCE represents the oxidation of U(V) to U(VI) (Liu et al., 2017). The small variation of the positions of these peaks compared with those in the literature could be attributed to the differences in over potentials of the different applied electrodes and the scan rates. Furthermore, the transferred charges of the oxidation and the reduction peaks were similar (Figure S13), suggesting no significant disproportionation of the U(V) upon its formation on the Ti electrode.

The precipitated U was further characterized to elucidate the PEC U extraction mechanisms. In the X-ray photoelectron spectroscopy (XPS) survey scan spectra, two characteristic U4f peaks emerged after the extraction (Figure 5C), indicating U deposition on the Ti electrode, consistent with the SEM-EDS results (Cui et al., 2021a, 2021b; Zhang et al., 2019). The mineralogical composition of the PEC extracted U was characterized by X-ray diffraction (XRD). As shown in Figure 5E, upon PEC U extraction, broad Bragg reflection peaks at 2θ = 28.55°, 33.09°, 47.50°, and 56.36° emerged, which could be assigned to uraninite structures. This finding suggests that the PEC extracted U is present in the form of uraninite. Although uraninite is nominally UO_2 with a fluorite-type (CaF_2) structure, its actual stoichiometry can vary significantly (UO_{2+x}, $0 \leq x \leq 0.61$) owing to the variance of the oxidation state of U (Janeczek and Ewing, 1992). XPS high-resolution U4f scan was then performed to further confirm the oxidation state of the extracted U. The spectrum shows two major peaks separated from each other by ~10.8 eV (Figure 5D). These two peaks could be assigned to the $U4f_{7/2}$ and $U4f_{5/2}$, respectively, and the separation of these two peaks was due to the spin-orbit split (Eloirdi et al., 2018). In addition, two small peaks at 399.7 and 388.8 eV were also observed (Figure 5D), which could be assigned to the satellite peaks of U(V) (Schindler et al., 2009; Eloirdi et al., 2018). Furthermore, the $U4f_{5/2}$ and $U4f_{7/2}$ peaks were fit (Schindler et al., 2009; Yuan et al., 2015a; Butorin et al., 2017), and the results show two strong peaks at 391.8 and 381.0 eV, both separated from their corresponding satellite peak by 7.8 eV. Although the primary peak-satellite peak separation for U(V) may vary slightly depending on the bonding environment, it is a powerful diagnostic tool for identifying U(V), and the 7.8–8.5 eV primary peak-satellite peak separation is a robust indicator of U(V) (Ilton et al., 2007; Yuan et al., 2015a; El Jamal et al., 2021; Butorin et al., 2017). Based on these data, the two U4f peaks could both be assigned to U(V) (Schindler et al., 2009; Yuan et al., 2015a; Butorin et al., 2017; Gouder et al., 2018; Eloirdi et al., 2018; El Jamal et al., 2021). The absence of spectral patterns of either U(VI) or U(IV) shows that the PEC extracted U was pentavalent, consistent with the CV characterization. Although some previous studies on the homogeneous photoreduction of U(VI) showed that the photosensitization of aqueous U(VI) may lead to the formation of U(V) (Tsushima et al., 2010; Haubitz et al., 2021; Li et al., 2019d), upon illumination aqueous U(V) is very unstable and prone to re-oxidation if halide ions and/or dissolved oxygen are present in the reaction solution (Haubitz et al., 2021; Tsushima et al., 2010). We examined the UV-vis absorption spectra of the reaction solution before and after illumination, and no characteristic peaks of U(V) were observed, suggesting no formation of stable U(V) via the homogeneous photosensitization pathway. Thus, the formation of U(V) via the photosensitization of aqueous U(VI) can be excluded. Alternatively, a few studies have shown that solid-phase U(V) could be stabilized by the surface where it is sorbed via coordination with the surface atoms (Yuan et al., 2015a, 2015b; Pan et al., 2020; Ilton et al., 2005; Pidchenko et al., 2017). For instance, Ilton et al. reported the formation of U(V) via heterogeneous reduction of aqueous U(VI) on the surface of ferrous mica surfaces, and the sorbed U(V) showed significantly better stability over a broad range of solution pH and ionic strength than aqueous U(V) obtained under the same conditions (Ilton et al., 2005). Pan et al. recently studied the heterogeneous reduction of aqueous U(VI) on the surface of magnetite and found the formation of stable U(V) on the surface of magnetite (Pan et al., 2020). In the present study, stable U(V) was only obtained on the Ti electrode upon PEC extraction experiments. Under the same conditions, the PC-extracted U on the TNA electrode was a mixture of U(IV) and U(VI) (Figure S15). Hence, it is reasonable to hypothesize that the Ti surface stabilized the U(V). Future studies on the interactions between the surface-sorbed U(V) and the Ti surface are needed to further elucidate the mechanisms of the stabilization of U(V) on the Ti surface on atomic level.

Recovery of extracted U from the Ti electrode

The recoverability of the extracted U on Ti electrode was evaluated. Both the physicochemical method and the electrochemical method were examined (see Figure S16). As shown in Figure S16, by the physicochemical method, the 0.1 M HCl could recover 66.3% of the extracted U. By applying a bias voltage, the elution of

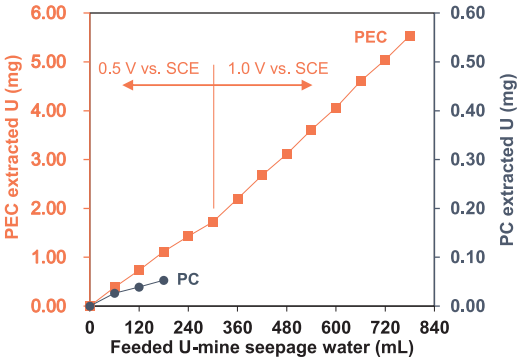

Figure 6. Long-term uranium extraction performances of the PEC method and the PC method during continuous cyclic runs in real uranium mine tailings seepage water

the extracted U could be promoted. In the 0.1 M HCl elution solution, the U recovery rate was 83.2% at 1.0 V bias voltage and 100.0% at 1.5 V, respectively. Therefore, the PEC-extracted U species on the Ti electrode could be fully recovered by applying a dilute acid and a low bias voltage.

U extraction in real U mine tailings seepage water

The U extraction performance of the proposed PEC method in real U mine seepage water was also evaluated, and the results are presented in Figure 6. The U extraction capacity of the PC method was only 0.04 gU $m^{-3}\cdot h^{-1}$, and it decreased dramatically to 0.02 gU $m^{-3}\cdot h^{-1}$ after only 2 cycles. For comparison, the PEC method extracted 5.54 mg U from 0.78 L seepage water after 13 cycles without noticeable efficiency decrease, revealing its exceptional stability and high efficiency with U mine seepage water compared with the PC method. The U extraction capacity is calculated to be 0.48 and 0.67 gU $m^{-3}\cdot h^{-1}$ at applied bias potentials of 0.5 and 1.0 V, respectively, which are 12–17 times higher than in the PC method. Moreover, the bias potential applied here served only as a driving force to separate the charge carriers (Figure S17). These results show that the PEC method has both higher U extraction efficiency and higher stability than the PC method in practical applications.

For the analysis of the feasibility of the proposed PEC U extraction method from the economic perspective, a cost-effective analysis is provided. We estimate that the cost for PEC U extraction from real U mine seepage water was $8.75/kgU and $15.63/kgU at 0.5 and 1.0 V bias potential, respectively. In comparison, for the conventional terrestrial U resources, the acceptable exploitation cost is $260/kgU (NEA & IAEA, 2021). Hence, the extraction of U from U mine tailings seepage water should be economically feasible.

DISCUSSION

On the global scale, a considerable amount of U is overlooked in over billions of tons of mine tailings and is released into the environment via seepage water (Dang et al., 2018). The present work successfully demonstrated the potential of the PEC method for U extraction from these seepage waters. For the U mine tailings where the studied seepage water was collected, the annual extractable U in the seepage water was 219–2,190 kg, which accounts for up to 1.5‰ of the annual gross domestic U production of China (NEA & IAEA, 2021). Given the obtained U extraction capacity (0.48–0.67 gU $m^{-3}\cdot h^{-1}$) of the PEC method, this amount of U is fully recoverable if the PEC method is implemented. There are more than 908 million m^3 U mine tailings distributed in 163 U mining sites around the world (IAEA, 2004); hence, if the PEC method proposed herein can be applied to all of them, the annually extractable U could reach up to 10.7% of the annual global U consumption by the nuclear power industry. This can largely hedge the risks of the global U supply chain, as well as reduce the negative environmental impacts of U mining industry.

Besides nuclear power, alternative renewable energies, e.g., wind, solar, and tidal energies, are also playing important roles in decarbonization. However, these non-nuclear alternative renewable energies are causing increasing load variability to the power grids due to their intermittent nature (Olauson et al., 2016), so it is of vital importance to implement energy storage technology to mitigate such fluctuations. For long-term energy storage, converting and storing intermitting renewable electricity in the form of energy-dense chemicals (e.g., H_2 gas, H_2O_2) is of particular interest to the energy sector (Tang et al., 2021). On average, the net electrical energy density of U is estimated to be 43.3 MWh/kgU. In comparison, the gross energy densities of concentrated H_2O_2 (70% concentrated) and H_2 gas, the state-of-art energy storage chemicals, were 0.58 and 33.35 kWh/kg, respectively (Tang et al., 2021). Hence, the net electrical power density of U is at least three and five orders of magnitude

higher than the gross energy of H_2 gas and concentrated H_2O_2, respectively. Therefore, U is an ideal candidate for power-to-chemical energy storage. For the PEC U extraction method, the compulsory energy input is calculated to be 70–125 kWh/kgU (Table S3), without further optimization, which is only 0.16%–0.29% of the energy density of the extracted U. This analysis implies that the PEC U extraction method has also great potential for energy storage applications.

Moreover, the proposed PEC method opens a new avenue toward the facile synthesis of U(V), an often "overlooked" U oxidation state. U(V) chemistry is important for elucidating the biogeochemical behaviors of U in the environment and understanding the properties of the f electrons of actinide ions (Molinas et al., 2021; Chen et al., 2005). And a facile U(V) synthesis method is useful for assisting future studies on the U(V) chemistry. In addition, because of its unique electronic structure (Zhang et al., 2021), stable U(V) materials is also highly desired for photocatalysis, magnetism, and energy storage applications (Nocton et al., 2008; Zhang et al., 2021). However, owing to fast disproportionation (Liu et al., 2017), U(V) species are usually very unstable (Li et al., 2017, 2019b, 2019c; Cui et al., 2020a). Attempts have been made by pioneers in synthesizing stable U(V), but the state-of-the-art methods are complicated and time consuming, requiring the addition of organic ligands, heating, high pressure, and/or high voltage (Tondreau et al., 2018; Zhang et al., 2021; Nocton et al., 2008; Arnold et al., 2012; El Jamal et al., 2021; Gouder et al., 2018; Chen et al., 2005). To our best knowledge, this study is the first in successfully producing stable U(V) from aqueous media without adding organic ligands, under ambient conditions and in open air. This would significantly facilitate future studies on U(V) chemistry.

Limitations of study

Here we have demonstrated efficient and durable uranium extraction from uranium mine seepage water. By applying a bias potential on the photocatalyst, the PEC method indeed enables much faster U extraction with exceptional stability, compared with the PC method operating under identical conditions: in real seepage water the PEC method achieves an extraction capacity of 0.67 gU $m^{-3} \cdot h^{-1}$ without deactivation for 156 h continuous operation, which is 17 times faster than the photocatalytic method. However, further optimizations of the proposed method can be done to further increase the energetic efficiency. Possible approaches include enlarging the ratio of the electrode surface to the reactor volume, modification of the photocatalyst to make better use of the solar light, and modification of the uranium deposition electrode to increase its selectivity.

In aqueous solutions, under ambient atmosphere, U(V) species is prone to re-oxidation, as documented in the literature. We have revealed in this work that stable U(V) can be produced via the reduction of aqueous U(VI) on the Ti electrode, under ambient atmosphere. Some previous studies have indicated that the surface of some minerals (e.g., micas, magnetite) could stabilize solid U(V). In this study, by comparing the valence states of the extracted U on different electrodes (namely, TNA and Ti), we hypothesized that the U(V) we obtained was stabilized by the Ti surface. However, more detailed structural information of the produced U(V) compound and the possible interactions between the U(V) species and the Ti surface at the U-Ti interface remain unknown. Further mechanistic investigations into these aspects are needed, to understand how the Ti surface induced the formation of stable U(V).

STAR★METHODS

Detailed methods are provided in the online version of this paper and include the following:

- KEY RESOURCES TABLE
- RESOURCE AVAILABILITY
  - Lead contact
  - Materials availability
  - Data and code availability
- METHOD DETAILS
  - Uranium extraction experiment
  - Characterizations
  - Cost-effectiveness analysis
  - Estimation of the global recoverable uranium in uranium mine tailings
  - Calculation of the energy density of uranium

SUPPLEMENTAL INFORMATION

Supplemental information can be found online at https://doi.org/10.1016/j.isci.2021.103230.

ACKNOWLEDGMENTS

This work was supported by the National Natural Science Foundation of China (No. 42077352), the Key Research and Development Program of Shaanxi Province (2019KW-044), and the Fundamental Research Funds for the Central Universities (No. 31020200QD024, No. 3102019JC007).

AUTHOR CONTRIBUTIONS

Conceptualization, Y.Y., F.C., Y.W., and Y.F.; formal analysis, Y.L., M.L., S.M., C.L., Y.C., Y.F., F.C., Y.Y., and Y.W.; funding acquisition, Y.Y., F.C., and Y.W.; investigation, J.J., Z.Q., and X.T.; methodology, Y.Y., F.C., and Y.W.; project administration, Y.Y., F.C., and Y.W.; resources, Y.Y., F.C., and Y.W.; supervision, Y.Y., F.C., and Y.W.; validation, Y.Y., F.C., and Y.W.; visualization, Y.Y.; writing – original draft, Y.Y.; writing – review & editing, F.C., Y.W., and Y.F.

DECLARATION OF INTERESTS

The authors declare no competing interests.

Received: August 10, 2021
Revised: September 8, 2021
Accepted: September 30, 2021
Published: November 19, 2021

REFERENCES

Arnold, P.L., Jones, G.M., Odoh, S.O., Schreckenbach, G., Magnani, N., and Love, J.B. (2012). Strongly coupled binuclear uranium–oxo complexes from uranyl oxo rearrangement and reductive silylation. Nat. Chem. *4*, 221–227.

Bonato, M., Ragnarsdottir, K.V., and Allen, G.C. (2012). Removal of Uranium(VI), lead(II) at the surface of TiO_2 nanotubes studied by X-ray photoelectron spectroscopy. Water Air Soil Pollut. *223*, 3845–3857.

Bourrachot, S., Brion, F., Pereira, S., Floriani, M., Camilleri, V., CAVALIÉ, I., Palluel, O., and Adam-Guillermin, C. (2014). Effects of depleted uranium on the reproductive success and F1 generation survival of zebrafish (*Danio rerio*). Aquat. Toxicol. *154*, 1–11.

Butorin, S.M., Kvashnina, K.O., Prieur, D., Rivenet, M., and Martin, P.M. (2017). Characteristics of chemical bonding of pentavalent uranium in La-doped UO_2. Chem. Commun. *53*, 115–118.

Chen, C.-S., Lee, S.-F., and Lii, K.-H. (2005). K(UO)Si_2O_6: a pentavalent−uranium silicate. J. Am. Chem. Soc. *127*, 12208–12209.

Chen, J., Zhang, L., Lam, Z., Tao, H.B., Zeng, Z., Yang, H.B., Luo, J., Ma, L., Li, B., Zheng, J., et al. (2016). Tunneling interlayer for efficient transport of charges in metal oxide electrodes. J. Am. Chem. Soc. *138*, 3183–3189.

Cui, W.-R., Li, F.-F., Xu, R.-H., Zhang, C.-R., Chen, X.-R., Yan, R.-H., Liang, R.-P., and Qiu, J.-D. (2020a). Regenerable covalent organic frameworks for photo-enhanced uranium adsorption from seawater. Angew. Chem. Int. Ed. *59*, 17684–17690.

Cui, W.-R., Zhang, C.-R., Jiang, W., Li, F.-F., Liang, R.-P., Liu, J., and Qiu, J.-D. (2020b). Regenerable and stable sp^2 carbon-conjugated covalent organic frameworks for selective detection and extraction of uranium. Nat. Commun. *11*, 436.

Cui, W.-R., Zhang, C.-R., Xu, R.-H., Chen, X.-R., Jiang, W., Li, Y.-J., Liang, R.-P., Zhang, L., and Qiu, J.-D. (2021a). Rational design of covalent organic frameworks as a groundbreaking uranium capture platform through three synergistic mechanisms. Appl. Catal. B Environ. *294*, 120250.

Cui, W.-R., Zhang, C.-R., Xu, R.-H., Chen, X.-R., Yan, R.-H., Jiang, W., Liang, R.-P., and Qiu, J.-D. (2021b). Low band gap benzoxazole-linked covalent organic frameworks for photo-enhanced targeted uranium recovery. Small *17*, 2006882.

Dang, D.H., Wang, W., Pelletier, P., Poulain, A.J., and Evans, R.D. (2018). Uranium dispersion from U tailings and mechanisms leading to U accumulation in sediments: insights from biogeochemical and isotopic approaches. Sci. Total Environ. *610-611*, 880–891.

Deng, H., Li, Z.-J., Wang, L., Yuan, L.-Y., Lan, J.-H., Chang, Z.-Y., Chai, Z.-F., and Shi, W.-Q. (2019). Nanolayered Ti_3C_2 and $SrTiO_3$ composites for photocatalytic reduction and removal of Uranium(VI). ACS Appl. Nano Mater. *2*, 2283–2294.

Dlamini, T.C., Tshivhase, V.M., Maleka, P., Penabei, S., and Mashaba, M. (2019). The effect of uranium speciation on the removal of gross alpha activity from acid mine drainage using anion exchange resin. J. Radioanal. Nucl. Chem. *319*, 357–363.

Eloirdi, R., Cakir, P., Huber, F., Seibert, A., Konings, R., and Gouder, T. (2018). X-ray photoelectron spectroscopy study of the reduction and oxidation of uranium and cerium single oxide compared to (U–Ce) mixed oxide films. Appl. Surf. Sci. *457*, 566–571.

Feng, Y., Rijnaarts, H.H.M., Yntema, D., Gong, Z., Dionysiou, D.D., Cao, Z., Miao, S., Chen, Y., Ye, Y., and Wang, Y. (2020). Applications of anodized TiO_2 nanotube arrays on the removal of aqueous contaminants of emerging concern: a review. Water Res. *186*, 116327.

Gao, H., Zhou, T., Zheng, Y., Zhang, Q., Liu, Y., chen, J., Liu, H., and Guo, Z. (2017). CoS quantum dot nanoclusters for high-energy potassium-ion batteries. Adv. Funct. Mater. *27*, 1702634.

Garcia-Segura, S., and Brillas, E. (2017). Applied photoelectrocatalysis on the degradation of organic pollutants in wastewaters. J. Photochem. Photobiol. C Photochem. Rev. *31*, 1–35.

Gouder, T., Eloirdi, R., and Caciuffo, R. (2018). Direct observation of pure pentavalent uranium in U_2O_5 thin films by high resolution photoemission spectroscopy. Sci. Rep. *8*, 8306.

Haubitz, T., Drobot, B., Tsushima, S., Steudtner, R., Stumpf, T., and Kumke, M.U. (2021). Quenching mechanism of Uranyl(VI) by chloride and bromide in aqueous and non-aqueous solutions. J. Phys. Chem. A *125*, 4380–4389.

Hennig, C., Ikeda-Ohno, A., Emmerling, F., Kraus, W., and Bernhard, G. (2010). Comparative investigation of the solution species $[U(CO_3)_5]^{6-}$ and the crystal structure of $Na_6[U(CO_3)_5]\cdot 12H_2O$. Dalton Trans. *39*, 3744–3750.

IAEA (2004). The Long Term Stabilization of Uranium Mill Tailings (International Atomic Energy Agency).

Ilton, E.S., Haiduc, A., Cahill, C.L., and Felmy, A.R. (2005). Mica surfaces stabilize pentavalent uranium. Inorg. Chem. *44*, 2986–2988.

Ilton, E.S., Boily, J.-F., and Bagus, P.S. (2007). Beam induced reduction of U(VI) during X-ray photoelectron spectroscopy: the utility of the U4f satellite structure for identifying uranium oxidation states in mixed valence uranium oxides. Surf. Sci. *601*, 908–916.

El Jamal, G., Gouder, T., Eloirdi, R., and Jonsson, M. (2021). X-ray and ultraviolet photoelectron spectroscopy studies of Uranium(iv), (v) and(vi) exposed to H_2O-plasma under UHV conditions. Dalton Trans. *50*, 729–738.

Janeczek, J., and Ewing, R.C. (1992). Structural formula of uraninite. J. Nucl. Mater. *190*, 128–132.

Kim, Y.K., Lee, S., Ryu, J., and Park, H. (2015). Solar conversion of seawater Uranium(VI) using TiO_2 electrodes. Appl. Catal. B Environ. *163*, 584–590.

Li, Z.-J., Huang, Z.-W., Guo, W.-L., Wang, L., Zheng, L.-R., Chai, Z.-F., and SHI, W.-Q. (2017). Enhanced photocatalytic removal of uranium(VI) from aqueous solution by magnetic TiO_2/Fe_3O_4 and its graphene composite. Environ. Sci. Technol. *51*, 5666–5674.

Li, P., Wang, J., Peng, T., Wang, Y., Liang, J., Pan, D., and Fan, Q. (2019a). Heterostructure of anatase-rutile aggregates boosting the photoreduction of U(VI). Appl. Surf. Sci. *483*, 670–676.

Li, P., Wang, J., Wang, Y., Liang, J., He, B., Pan, D., Fan, Q., and Wang, X. (2019b). Photoconversion of U(VI) by TiO_2: an efficient strategy for seawater uranium extraction. Chem. Eng. J. *365*, 231–241.

Li, P., Wang, J., Wang, Y., Liang, J., Pan, D., Qiang, S., and Fan, Q. (2019c). An overview and recent progress in the heterogeneous photocatalytic reduction of U(VI). J. Photochem. Photobiol. C Photochem. Rev. *41*, 100320.

Li, Y., Rizvi, S.A.-E.-A., Hu, D., Sun, D., Gao, A., Zhou, Y., LI, J., and JIANG, X. (2019d). Selective late-stage oxygenation of sulfides with ground-state oxygen by uranyl photocatalysis. Angew. Chem. Int. Ed. *58*, 13499–13506.

Li, H., CHAO, D., Chen, B., Chen, X., Chuah, C., Tang, Y., Jiao, Y., Jaroniec, M., and Qiao, S.-Z. (2020). Revealing principles for design of lean-electrolyte lithium metal anode via in situ spectroscopy. J. Am. Chem. Soc. *142*, 2012–2022.

Li, D., Dai, L., Ren, X., Ji, F., Sun, Q., Zhang, Y., and Ci, L. (2021). Foldable potassium-ion batteries enabled by free-standing and flexible SnS2@C nanofibers. Energy Environ. Sci. *14*, 424–436.

Liang, P.-L., Yuan, L.-Y., Deng, H., Wang, X.-C., Wang, L., LI, Z.-J., Luo, S.-Z., and Shi, W.-Q. (2020). Photocatalytic reduction of Uranium(VI) by magnetic $ZnFe_2O_4$ under visible light. Appl. Catal. B Environ. *267*, 118688.

Lianos, P. (2017). Review of recent trends in photoelectrocatalytic conversion of solar energy to electricity and hydrogen. Appl. Catal. B Environ. *210*, 235–254.

Liu, C., Hsu, P.-C., Xie, J., Zhao, J., Wu, T., Wang, H., Liu, W., Zhang, J., Chu, S., and Cui, Y. (2017). A half-wave rectified alternating current electrochemical method for uranium extraction from seawater. Nat. Energy *2*, 17007.

Liu, T., Yuan, J., Zhang, B., Liu, W., Lin, L., Meng, Y., Yin, S., Liu, C., and Luan, F. (2019). Removal and recovery of uranium from groundwater using direct electrochemical reduction method: performance and implications. Environ. Sci. Technol. *53*, 14612–14619.

Lively, D.S.S.R.P. (2016). Seven chemical separations to change the world. Nature *532*, 435–437.

Mazierski, P., Borzyszkowska, A.F., Wilczewska, P., Białk-Bielińska, A., Zaleska-Medynska, A., Siedlecka, E.M., and Pieczyńska, A. (2019). Removal of 5-fluorouracil by solar-driven photoelectrocatalytic oxidation using Ti/TiO_2(NT) photoelectrodes. Water Res. *157*, 610–620.

Molinas, M., Faizova, R., Brown, A., Galanzew, J., Schacherl, B., Bartova, B., Meibom, K.L., Vitova, T., Mazzanti, M., and Bernier-Latmani, R. (2021). Biological reduction of a U(V)–Organic ligand complex. Environ. Sci. Technol. *55*, 4753–4761.

Morris, D.E. (2002). Redox energetics and kinetics of uranyl coordination complexes in aqueous solution. Inorg. Chem. *41*, 3542–3547.

NEA & IAEA (2021). Uranium 2020 (OECD Publishing).

Nocton, G., Horeglad, P., Pécaut, J., and Mazzanti, M. (2008). Polynuclear cation−cation complexes of pentavalent uranyl: relating stability and magnetic properties to structure. J. Am. Chem. Soc. *130*, 16633–16645.

Olauson, J., Ayob, M.N., Bergkvist, M., Carpman, N., Castellucci, V., Goude, A., Lingfors, D., Waters, R., and Widén, J. (2016). Net load variability in Nordic countries with a highly or fully renewable power system. Nat. Energy *1*, 16175.

Pan, Z., Bártová, B., Lagrange, T., Butorin, S.M., Hyatt, N.C., Stennett, M.C., Kvashnina, K.O., and Bernier-Latmani, R. (2020). Nanoscale mechanism of UO_2 formation through uranium reduction by magnetite. Nat. Commun. *11*, 4001.

Pidchenko, I., Kvashnina, K.O., Yokosawa, T., Finck, N., Bahl, S., Schild, D., polly, R., Bohnert, E., Rossberg, A., Göttlicher, J., et al. (2017). Uranium redox transformations after U(VI) coprecipitation with magnetite nanoparticles. Environ. Sci. Technol. *51*, 2217–2225.

Radecka, M. (2004). TiO_2 for photoelectrolytic decomposition of water. Thin Solid Films *451–452*, 98–104.

Rhodes, R. (2017). More nuclear power can speed CO_2 cuts. Nature *548*, 281.

Schindler, M., Hawthorne, F.C., Freund, M.S., and Burns, P.C. (2009). XPS spectra of uranyl minerals and synthetic uranyl compounds. I: the U 4f spectrum. Geochim. Cosmochim. Acta *73*, 2471–2487.

Tang, J., Zhao, T., Solanki, D., Miao, X., Zhou, W., and Hu, S. (2021). Selective hydrogen peroxide conversion tailored by surface, interface, and device engineering. Joule *5*, 1432–1461.

Tondreau, A.M., Duignan, T.J., Stein, B.W., Fleischauer, V.E., Autschbach, J., Batista, E.R., Boncella, J.M., Ferrier, M.G., Kozimor, S.A., Mocko, V., et al. (2018). A pseudotetrahedral Uranium(V) complex. Inorg. Chem. *57*, 8106–8115.

Tsouris, C. (2017). Uranium extraction: fuel from seawater. Nat. Energy *2*, 17022.

Tsushima, S., Götz, C., and Fahmy, K. (2010). Photoluminescence of Uranium(VI): quenching mechanism and role of Uranium(V). Chem. A Eur. J. *16*, 8029–8033.

Wang, M., Ioccozia, J., SUN, L., LIN, C., and LIN, Z. (2014). Inorganic-modified semiconductor TiO_2 nanotube arrays for photocatalysis. Energy Environ. Sci. *7*, 2182–2202.

Wang, Z., Meng, Q., Ma, R., Wang, Z., Yang, Y., Sha, H., Ma, X., Ruan, X., Zou, X., Yuan, Y., and Zhu, G. (2020). Constructing an ion pathway for uranium extraction from seawater. Chem *6*, 1683–1691.

Yang, H.G., Sun, C.H., Qiao, S.Z., Zou, J., Liu, G., Smith, S.C., Cheng, H.M., and Lu, G.Q. (2008). Anatase TiO_2 single crystals with a large percentage of reactive facets. Nature *453*, 638–641.

Yuan, K., Ilton, E.S., Antonio, M.R., Li, Z., Cook, P.J., and Becker, U. (2015a). Electrochemical and spectroscopic evidence on the one-electron reduction of U(VI) to U(V) on magnetite. Environ. Sci. Technol. *49*, 6206–6213.

Yuan, K., Renock, D., Ewing, R.C., and Becker, U. (2015b). Uranium reduction on magnetite: probing for pentavalent uranium using electrochemical methods. Geochim. Cosmochim. Acta *156*, 194–206.

Yuan, Y., Yu, Q., Cao, M., Feng, L., Feng, S., Liu, T., Feng, T., Yan, B., Guo, Z., and Wang, N. (2021). Selective extraction of uranium from seawater with biofouling-resistant polymeric peptide. Nat. Sustain. *4*, 708–714.

Zhang, Z., and Yates, J.T. (2012). Band bending in semiconductors: chemical and physical consequences at surfaces and interfaces. Chem. Rev. *112*, 5520–5551.

Zhang, H., Liu, W., Li, A., Zhang, D., Li, X., Zhai, F., Chen, L., Chen, L., Wang, Y., and Wang, S. (2019). Three mechanisms in one material: uranium capture by a polyoxometalate–organic framework through combined complexation, chemical reduction, and photocatalytic reduction. Angew. Chem. Int. Ed. *58*, 16110–16114.

Zhang, M., Liang, C., Cheng, G.-D., Chen, J., Wang, Y., He, L., Cheng, L., Gong, S., Zhang, D., Li, J., et al. (2021). Intrinsic semiconducting behavior in a large mixed-valent uranium(V/VI) cluster. Angew. Chem. Int. Ed. *60*, 9886–9890.

Zheng, M., Ji, H., Duan, J., Dang, C., Chen, X., and Liu, W. (2020). Efficient adsorption of Europium(III) and Uranium(VI) by titanate nanorings: insights into radioactive metal species. Environ. Sci. Ecotechnol. *2*, 100031.

STAR★METHODS

KEY RESOURCES TABLE

REAGENT or RESOURCE	SOURCE	IDENTIFIER
Chemicals, peptides, and recombinant proteins		
Soudium Nitrate (Analytical grade)	Shanghai Chemical Reagent Co., Ltd	CAS: 7631-99-4
Hydrochloric Acid (Analytical grade)	Shanghai Chemical Reagent Co., Ltd	CAS: 7647-01-0
Arsenazo III (Analytical grade)	Macklin	CAS: 1668-00-4
Sodium Hydroxide (Analytical grade)	Shanghai Chemical Reagent Co., Ltd	CAS: 1310-73-2
Titanium foil (0.3 mm thickness, 99.7%)	Haiyuan	CAS: 7740-32-6
Uanyl Nitrate Hexahydrate (Analytical grade)	Hubei Qifei Chemical Co., Ltd	CAS: 13520-83-7
Sodium Chloride (Analytical grade)	Shanghai Chemical Reagent Co., Ltd	CAS: 7647-14-5
Sodium Sulfate Anhydrous (Analytical grade)	Macklin	CAS: 7757-82-6
Software and algorithms		
Visual MINTEQ 3.1	KTH	https://vminteq.lwr.kth.se/
Nova 2.1.3	Metrohm Autolab	https://www.metrohm-autolab.com/news/NOVA213.html
Other		
Shimadzu UV-1780 UV-Visible Spectrophotometer	Shimadzu	https://www.shimadzu.com.cn/an/spectro/uv/uv-1780/2136.html
Hitachi SU8010 Scanning Electron Microscope	Hitachi	https://www.hitachi-hightech.com/file/ca/pdf/library/literature/SU8000FamilyBrochure.pdf
Thermo Scientific™K-Alpha+X-ray photoelectron spectrometer	Thermo Scientific	https://tools.thermofisher.com/content/sfs/brochures/BR52586_E_0714M_K-AlphaPlus_web_H_2.pdf#:~:text=The%20Thermo%20Scientific%E2%84%A2K-Alpha%2BX-ray%20photoelectron%20spectrometer%20features%20a%20low,the%20feature%20of%20interest%20to%20maximize%20the%20signal.
Rigaku D Max 2500 Pc Powder X Ray Diffractometer	Rigaku	https://www.rigaku.com/products/xrd/smartlab
CHI660E Electrochemical Workstation	Shanghai Chenhua	http://www.chinstr.com/product/274590875

RESOURCE AVAILABILITY

Lead contact

Further information and requests for resources should be directed to and fulfilled by the lead contact, Yin Ye (yeyin01@hotmail.com; yin.ye@nwpu.edu.cn).

Materials availability

This study did not generate new unique reagents.

Data and code availability

- All data reported in this paper will be shared by the lead contact upon request.
- This paper does not report original code.
- Any additional information required to reanalyze the data reported in this paper is available from the lead contact upon request.

METHOD DETAILS

Uranium extraction experiment

U extraction experiments were carried out using a single-compartment three-electrode reactor, which has an effective volume of 0.06 L. A 3 cm × 3 cm TiO_2 nanotube array (TNA) was used as the anode (Figure S1), as TiO_2 is the most developed and most commonly used model photocatalyst (Yang et al., 2008), and its conduction band edge potential is suitable for U(VI) reduction (Li et al., 2017). A 3 cm × 3.5 cm Ti foil was used as the cathode, because its capability of serving as the U deposition site has been demonstrated in previous electrochemical uranium extraction studies (Liu et al., 2019). A saturated calomel electrode (SCE) was used as the reference electrode. An electrochemical workstation (CHI660E) was used to provide the designated bias on the TNA anode, and a UV-LED array with 60 mW/cm^2 irradiation was used as the light source. In the case of the PC method, the reactor was operated at open-cell conditions without circuit connection between the TNA anode and the Ti electrode under illumination. In the case of the EC method, the system was operated in dark at designated bias potentials. Synthetic U-containing water was made by dissolving $UO_2(NO_3)_2{\cdot}6H_2O$ into ultra-pure water to reach desired concentrations. Meanwhile, 20 mM NaCl was also added as the supporting electrolyte, unless otherwise stated. For the real U-mine tailings seepage water experiments, seepage water collected from a decommissioned granite-related U mine tailings deposit was used after filtration by 0.2 μm filter membrane to remove suspended solids and microorganisms which may interfere the measurements. Detailed characterizations of the seepage water can be seen in Table S2. Upon each cycle (12 h) of the real U-mine tailings seepage water experiment, fresh Ti cathode was used while the TNA was continuously used without any means of regeneration. All experiments were conducted in the open-air. The U concentration was measured by a well-established spectrophotometric method as described in the literature (Kim et al., 2015). The extracted mass of the U was calculated by comparing the difference between the remaining and the initial U concentration in the reaction solution.

For the uranium recovery from the Ti electrode, a two-chamber (40 mL: 40 mL) two-electrode electrochemical reactor was used (Figure S16). The desorption experiments were carried out under open-circuit conditions (physicochemical desorption), 1.0 V bias voltage, and 1.5 V bias voltage. For each desorption experiment, samples were taken from the anodic chamber to examine the uranium concentration in the electrolyte (0.1 M HCl).

Characterizations

Cyclic voltammetry (CV) characterizations of the Ti electrode were carried out using the CHI660E electrochemical workstation, with a 4 cm × 3 cm graphite plate as the counter electrode and a SCE reference electrode. Scanning electron microscopy (SEM) and energy dispersive spectroscopy (EDS) were conducted using a SU8010 ultra-high-resolution FE-SEM equipped with an X-Max N EDS system. X-ray photoelectron spectroscopy (XPS) was carried out using a Thermo K-Alpha+ XPS with an Al (Kα) source. X-ray diffraction (XRD) (Rigaku D-Max 2500PC) was carried out using Cu Kα radiation.

Cost-effectiveness analysis

Considering the fact that the artificial light source can be omitted when solar light is employed as the light source, so the compulsory artificial energy input in the PEC method is the electricity consumption due to the application of the bias potential. So, the electrical energy input for the PEC extraction of uranium can be calculated based on the following equation:

$$E_{in} = \frac{1000 \times U_{cell}}{(C_t - C_0) \times V_{cell}} \int_0^t I\, dt \qquad \text{(Equation 1)}$$

Where E_{in} (kWh/kg-uranium) represents the electricity required for the extraction of per unit mass uranium, U_{cell} (V) is the voltage between the TNA anode and the Ti cathode under certain applied bias potential, I (A) is the recorded current under the applied bias potential without light illumination to exclude the current derived from photocatalytic process, C_t represents the uranium concentration (mg/L) at time t (h), C_0 represents the initial uranium concentration (mg/L), V_{cell} is the volume of the treated seepage water (L). If the current I reaches steady-state fast and is stable throughout the reaction, this equation can be then simplified to the following form:

$$E_{in} = \frac{1000 \times U_{cell} \times I_s \times t}{(C_t - C_0) \times V_{cell}} \qquad \text{(Equation 2)}$$

Where I_s (A) is the measured steady-state current under the applied bias potential. The electricity price for industrial users in China (~$0.125/kWh) was used to compute the operation cost.

Estimation of the global recoverable uranium in uranium mine tailings

Due to the lack of statistics of the global uranium mine tailings reservation and the characteristics and amount of the seepage water derived, it is difficult to accurately assess the annually recoverable uranium from mine tailings on the global scale. Hence, we hereby provide a rough estimation. For the mine tailings (volume = 313000 m^3) we studied herein, annually 219~2190 kgU was extractable. We therefore assume that on average the annual extractable uranium from per unit volume mine tailings was 0.0007~0.0070 kgU/m^3-tailings. According to a report by IAEA on the global uranium mine tailings, there were 908 million m^3 U mine tailings distributed in 163 U mining sites around the world (IAEA, 2004), so globally the annually extractable uranium from these tailings was approximately 635310~6353100 kgU (635.31~6353.1tU). The annual global uranium consumption by the nuclear power industry was 59200 tU (according recent statistical data by IAEA (NEA & IAEA, 2021)), so the extractable uranium in tailings could be calculated to meet 1.07%~10.7% of the global nuclear power related uranium demand.

Calculation of the energy density of uranium

Calculation of the electricity generation capacity (i.e. energy density) of uranium was based on the world annual nuclear power reactor-related uranium consumption data and the global annual nuclear power production data provided in a recent joint statistics report published by the Nuclear Energy Agency (NEA) and the International Atomic Energy Agency (IAEA) (NEA & IAEA, 2021). In detail, as of January 2019, the statistics data show an annual world reactor-related uranium consumption of 59200 tU in the year of 2018, while a gross global net electricity generation from nuclear power industry was 2562.7 TWh in the same year. So it can be easily calculated from these data that the net electricity generation capacity of U is 43.3 GWh/tU (i.e. 43.3 MWh/kgU), by dividing the electricity generation data by the U consumption data.